Intermolecular Activation of Hydrocarbon C−H Bonds Initiated by the Tungsten Hydrocarbyl Hydrido Complexes Cp*W(NO)(R)(H)(PMe_3) (R = Alkyl, Aryl)

Kajin Lee,[†] Peter Legzdins,*[,†] Craig B. Pamplin,[†] Brian O. Patrick,[†] and Kenji Wada[‡]

Department of Chemistry, The University of British Columbia, Vancouver, British Columbia, Canada V6T 1Z1, and Department of Energy and Hydrocarbon Chemistry, Graduate School of Engineering, Kyoto University, Katsura, Nishikyo-ku, Kyoto 615-8510, Japan

Received November 9, 2004

trans-Cp*W(NO)(CH_2EMe_3)(H)(PMe_3) (E = C, Si) complexes can be prepared by the hydrogenation at 1 atm of the appropriate Cp*W(NO)(CH_2EMe_3)$_2$ precursor in the presence of a slight excess of PMe_3. (Our designation of a particular geometrical isomer as cis or trans in this family of complexes indicates the relative positions of the hydrocarbyl and the hydrido ligands in the base of a four-legged piano-stool molecular structure.) The use of D_2 in place of H_2 during these syntheses affords the corresponding *trans*-Cp*W(NO)(CH_2EMe_3)(D)(PMe_3) (E = C, Si) complexes. The *cis*-Cp*W(NO)(CH_2EMe_3)(H)(PMe_3) isomers are obtainable by C−H bond-activation reactions of the trans precursors. Thus, activation of $SiMe_4$ by *trans*-Cp*W(NO)(CH_2CMe_3)(H)(PMe_3) under ambient conditions produces *cis*-Cp*W(NO)(CH_2SiMe_3)(H)(PMe_3). Similarly, activations of C_6H_6 and C_6D_6 at 20−27 °C by the *trans*-Cp*W(NO)(CH_2EMe_3)(H)(PMe_3) complexes produce *cis*-Cp*W(NO)(C_6H_5)(H)(PMe_3) and *cis*-Cp*W(NO)(C_6D_5)(D)(PMe_3), respectively, and the solid-state molecular structure of the latter complex has been established by a single-crystal X-ray crystallographic analysis. Kinetic, mechanistic, and theoretical investigations of these benzene C−H activation processes are consistent with initial trans to cis isomerization of the reactants followed by intramolecular reductive elimination of EMe_4 to form the 16-electron Cp*W(NO)(PMe_3) intermediate. Subsequent oxidative addition of the incoming benzene substrate to this coordinatively unsaturated intermediate produces the final cis hydrido phenyl complex. These single C−H activation processes are the requisite first steps in the development of these organometallic complexes as catalysts for the selective functionalization of hydrocarbons. All new complexes have been characterized by conventional spectroscopic methods.

Introduction

Interest in C−H bond activations at transition-metal centers continues unabated, since these processes hold the promise of leading to efficient and catalytic methods for the selective conversion of hydrocarbon feedstocks into functionalized organic compounds.[1] Considerable progress in this regard has been made in the past 20 years, and numerous metal-containing complexes have been discovered to effect intermolecular C−H bond activations, often selectively under relatively mild conditions.[2] Notable examples include (1) late-transition-metal complexes that oxidatively add C−H linkages to the metal center, (2) transition-metal, lanthanide, and actinide complexes that facilitate C−H activation via M−C σ-bond metathesis, and (3) early- to mid-transition-metal complexes that add C−H bonds across M=N and M=C linkages. A fundamental understanding of these discrete C−H activation processes has been acquired for many of these complexes, and the chemistry of select systems has been significantly advanced toward efficient, catalytic functionalizations.[2]

Our contributions to this area of chemistry began with our recent discovery that Cp*M(NO)(hydrocarbyl)$_2$ complexes (Cp* = η^5-C_5Me_5) of molybdenum and tungsten exhibit hydrocarbyl-dependent thermal chemistry.[3] Thus, gentle thermolysis of appropriate Cp*M(NO)(hydrocarbyl)$_2$ precursors (M = Mo, W) results in loss of hydrocarbon and the transient formation of 16-electron organometallic complexes such as Cp*M(NO)(alkylidene), Cp*M(NO)(η^2-allene), and Cp*M(NO)(η^2-benzyne). These intermediates first effect the single activation of hydrocarbon C−H bonds intermolecularly via the reverse of the transformations by which they were generated. Some of the new product complexes formed in this manner are stable and may be isolated. Others are thermally unstable under the experimental conditions employed and react further to effect double or triple C−H bond activations of the hydrocarbon substrates.

* To whom correspondence should be addressed. E-mail: legzdins@chem.ubc.ca.
[†] University of British Columbia.
[‡] Kyoto University.

(1) (a) Crabtree, R. H. *Dalton* **2001**, 2437. (b) Fekl, U.; Goldberg, K. I. *Adv. Inorg. Chem.* **2003**, *54*, 529 and references therein.

(2) (a) Labinger, J. A.; Bercaw, J. E. *Nature* **2002**, *417*, 507 and references therein. (b) *Activation and Functionalization of C−H Bonds*; Goldberg, K. I., Goldman, A. S., Eds.; ACS Symposium Series 885; American Chemical Society: Washington, DC, 2004, and various chapters contained therein.

(3) Pamplin, C. B.; Legzdins, P. *Acc. Chem. Res.* **2003**, *36*, 223.

10.1021/om049137e CCC: $30.25
Publication on Web 01/11/2005

Even though the 16-electron organometallic intermediates responsible for these C−H activation processes have not been detected spectroscopically, their existence has been inferred from the fact that they can usually be trapped as 18-electron adducts by Lewis bases such as pyridine and PMe_3.[3] However, once trapped, they generally lose the ability to initiate C−H bond activations. The one notable exception to this generalization is provided by the 18-electron adduct *trans*-Cp*W(NO)(CH_2SiMe_3)(H)(PMe_3),[4] which can effect the single C−H bond activation of benzene, a discovery made in connection with other studies in these laboratories 17 years ago.[5] Intrigued by the apparently unique behavior of this alkyl hydrido complex of tungsten, we decided to investigate it and its neopentyl analogue, *trans*-Cp*W(NO)(CH_2CMe_3)(H)(PMe_3), more fully in light of our recent experiences with the other C−H-activating nitrosyl complexes of molybdenum and tungsten.[3] In this report, we present the results of our experimental and theoretical investigations of the C−H activation chemistry of the *trans*-Cp*W(NO)(CH_2EMe_3)(H)(PMe_3) (E = C, Si) compounds and contrast it with that exhibited by the well-studied 16-electron Cp*W(NO)(CH_2EMe_3)$_2$ (E = C, Si) precursor complexes.

Results and Discussion

Synthesis and Characterization of *trans*-Cp*W(NO)(CH_2EMe_3)(H)(PMe_3) (E = C, Si) Reactants. Both of the reactants having trans alkyl and hydrido ligands can be prepared in a similar manner, namely by the hydrogenation at 1 atm of the appropriate Cp*W(NO)(CH_2EMe_3)$_2$ (E = C, Si) precursor in the presence of a slight excess of PMe_3 (eq 1). The neopentyl complex

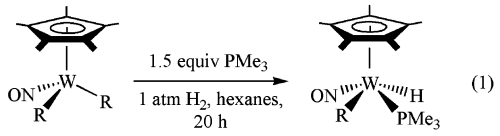

is new, but its (trimethylsilyl)methyl analogue was synthesized some time ago in our laboratories under the slightly more forcing conditions of 5.5 atm of H_2.[5] Orange-yellow *trans*-Cp*W(NO)(CH_2CMe_3)(H)(PMe_3) is air-stable in the solid state and is readily soluble in most common organic solvents. Its IR spectrum in Nujol exhibits a strong ν_{NO} absorption at 1543 cm^{-1} and a weak ν_{WH} band at 1851 cm^{-1}. The mass spectrum of an analytically pure sample of this compound displays a complex tungsten isotopic pattern centered around *m/z* 497, which corresponds to the parent ion.

The ^{1}H NMR spectrum of *trans*-Cp*W(NO)(CH_2CMe_3)(H)(PMe_3) in C_6D_6 has distinctive signals characteristic of a monomeric alkyl hydride complex. The signals due to the α-C protons of the alkyl group and the hydride exhibit the expected coupling patterns, but the signals of one of the α-C protons are obscured by the PMe_3 signal, a fact confirmed by HMQC spectroscopy. In addition, ^{1}H-selective NOE spectroscopy establishes that the hydride and the alkyl ligands of *trans*-Cp*W(NO)(CH_2CMe_3)(H)(PMe_3) are indeed in a trans configuration in its solution-state molecular structure. This trans configuration is consistent with the configuration previously established for *trans*-Cp*W(NO)(CH_2SiMe_3)(H)(PMe_3).[5] The use of D_2 in place of H_2 during conversions (1) produces the analogous monodeuteride complexes, which have also been fully characterized by conventional spectroscopic methods.

Scheme 1

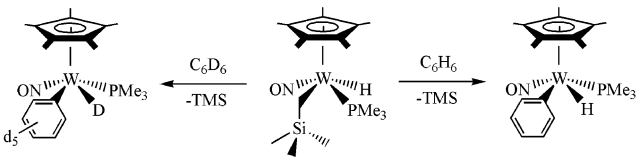

The cis alkyl hydride version of Cp*W(NO)(CH_2SiMe_3)(H)(PMe_3) can be synthesized via the C−H activation of tetramethylsilane (TMS) by *trans*-Cp*W(NO)(CH_2CMe_3)(H)(PMe_3) under ambient conditions (eq 2).

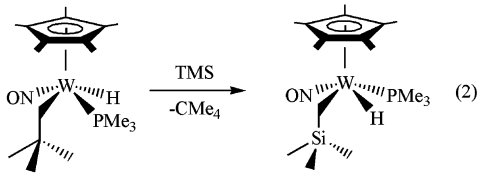

The cis configuration of the hydride and the alkyl groups in the product has again been established by ^{1}H-selective NOE spectroscopy. This cis configuration is consistent with the proposed mechanism of C−H bond activation by these complexes, in which the incoming alkane substrate oxidatively adds to the coordinatively unsaturated Cp*W(NO)(PMe_3) intermediate (vide infra).

Preparation and Characterization of Cp*W(NO)(C_6H_5)(H)(PMe_3) and Cp*W(NO)(C_6D_5)(D)(PMe_3). The C−H bond activation of benzene by *trans*-Cp*W(NO)(CH_2SiMe_3)(H)(PMe_3) was discovered in these laboratories in 1987,[5] and the *cis*-Cp*W(NO)(C_6H_5)(H)(PMe_3) product was characterized at that time by mass spectrometry and by ^{1}H NMR and IR spectroscopy. In addition to characterizing this complex more fully during the present investigations, we have also now discovered that effecting these C−H and C−D activations at 20−27 °C (rather than at 40 °C as previously) for longer periods of time results in generally cleaner reactions, although Cp*W(NO)(PMe_3)$_2$ and some intractable byproducts are still formed. Furthermore, the *cis*-Cp*W(NO)(C_6D_5)(D)(PMe_3) product apparently does not persist at the higher reaction temperature. These C−H and C−D bond activations proceed with the stereochemistry summarized in Scheme 1.

The cis phenyl deuteride configuration of *cis*-Cp*W(NO)(C_6D_5)(D)(PMe_3) in the solid state has been confirmed by a single-crystal X-ray crystallographic analysis (Figure 1). Again, this configuration supports the proposed mechanism for C−H bond activations by these complexes (vide infra). The metrical parameters of *cis*-Cp*W(NO)(C_6D_5)(D)(PMe_3) are normal and resemble those exhibited by other related tungsten nitrosyl complexes having distorted four-legged piano-stool mo-

(4) Throughout this report the designation of a particular geometrical isomer as cis or trans in this family of complexes indicates the relative positions of the hydrocarbyl and the hydrido ligands in the base of a four-legged piano-stool molecular structure.

(5) Legzdins, P.; Martin, J. T.; Einstein, F. W. B.; Jones, R. H. *Organometallics* **1987**, *6*, 1826.

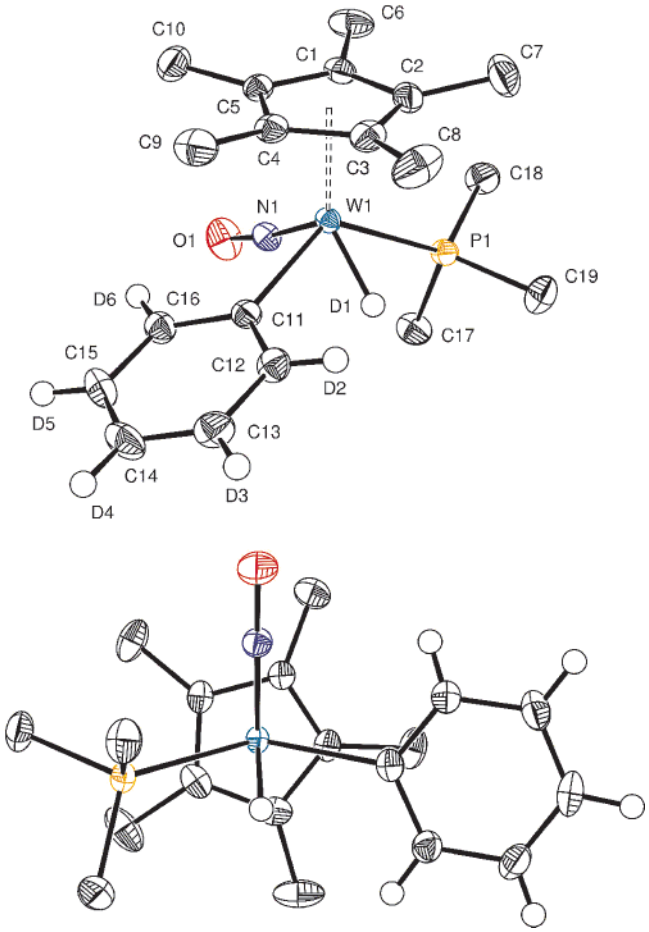

Figure 1. Two views of the solid-state molecular structure of *cis*-Cp*W(NO)(C_6D_5)(D)(PMe_3) with 50% probability ellipsoids. Selected bond lengths (Å) and angles (deg): W(1)−D(1) = 1.51(3), W(1)−C(11) = 2.1968(19), W(1)−P(1) = 2.4557(5), W(1)−N(1) = 1.7831(15), N(1)−O(1) = 1.222(2); W(1)−N(1)−O(1) = 172.82(15), C(11)−W(1)−D(1) = 68.6(12), W(1)−C(11)−C(12) = 123.90(15), W(1)−P(1)−C(18) = 121.52(8), P(1)−W(1)−C(11) = 126.93(5).

lecular structures.[5] Specifically, the C(11)−W(1)−D(1) angle is 68.6(12)°, and the short W−N (1.7831(15) Å) and long N−O (1.222(2) Å) bond lengths in its essentially linear WNO group indicate the existence of considerable W→NO back-bonding.[6]

Like other members of this family of complexes, yellow *cis*-Cp*W(NO)(C_6H_5)(H)(PMe_3) is soluble in common organic solvents, and its mass spectrum exhibits a complex tungsten isotopic pattern centered around *m/z* 425, which can be assigned to the fragment ion produced by the loss of C_6H_6 from the parent ion.

There is one interesting experimental aspect about the C−H and C−D bond activations of C_6H_6 and C_6D_6 summarized in Scheme 1, and that is that chromatography of the final reaction mixtures on silica with 1:1 hexanes/diethyl ether affords purple eluates which on cooling deposit clear yellow crystals of the desired products. The purple color of the eluates is evidently due to small amounts of side products, which are very soluble in all organic solvents. The purple products have so far eluded isolation and characterization, since only minuscule amounts of them are formed in addition to

(6) Chisholm, M. H.; Cotton, F. A.; Extine, M. W.; Kelly, R. L. *Inorg. Chem.* **1979**, *18*, 116 and references therein.

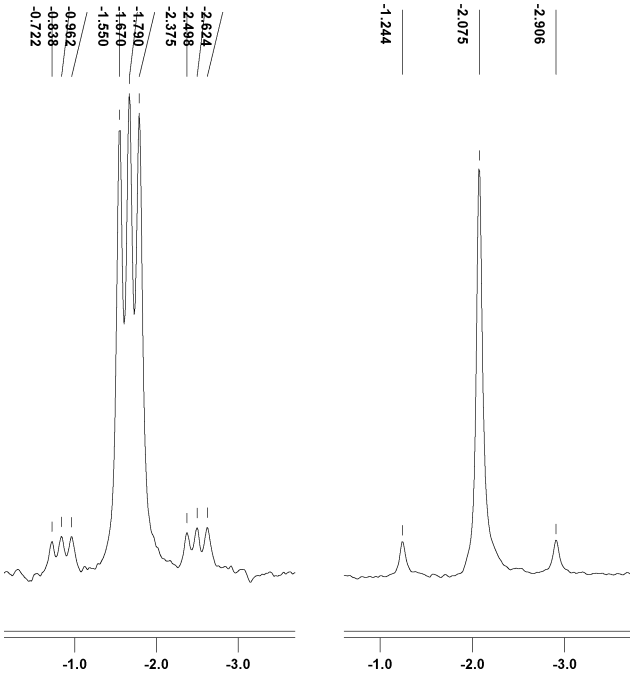

Figure 2. $^{31}P\{^1H\}$ NMR spectra of C_6D_6 solutions of *cis*-Cp*W(NO)(C_6D_5)(D)(PMe_3) (left) and *cis*-Cp*W(NO)(C_6H_5)(H)(PMe_3) (right).

the customary side products such as Cp*W(NO)(PMe_3)$_2$ and several intractable species.

As expected, a solution of *cis*-Cp*W(NO)(C_6D_5)(D)(PMe_3) in C_6D_6 displays the characteristic triplet signal with W−P coupling in its $^{31}P\{^1H\}$ NMR spectrum (Figure 2). (The analogous $^{31}P\{^1H\}$ NMR spectrum of *cis*-Cp*W(NO)(C_6H_5)(H)(PMe_3) is also shown in Figure 2 for comparison.) The ^1H NMR spectrum of *cis*-Cp*W(NO)(C_6D_5)(D)(PMe_3) in C_6D_6 exhibits the customary signals due to its Cp* and PMe_3 protons. This air-stable complex is soluble in common organic solvents, and its mass spectrum displays a tungsten isotopic pattern centered around *m/z* 425, which can be attributed to $[Cp^*W(NO)(PMe_3)]^+$. In its IR spectrum in Nujol, this compound exhibits a weak ν_{WD} absorption at 1261 cm^{-1} and a strong ν_{NO} absorption at 1567 cm^{-1}. For comparison, the Nujol-mull IR spectrum of *cis*-Cp*W(NO)(C_6H_5)(H)(PMe_3) displays a weak ν_{WH} absorption at 1812 cm^{-1} and a strong ν_{NO} absorption at 1550 cm^{-1}. The observed shift ν_{WH}/ν_{WD} is 1.4 and indicates that ν_{WH} and ν_{NO} are not strongly coupled for this hydrido complex.

In closing this section, some other observations concerning these benzene C−H activation processes merit mention. First, the C−D bond activation of C_6D_6 by *trans*-Cp*W(NO)(CH_2CMe_3)(H)(PMe_3) produces *cis*-Cp*W(NO)(C_6D_5)(D)(PMe_3) instead of *cis*-Cp*W(NO)(C_6D_5)(H)(PMe_3). This observation confirms that the hydride ligand of *cis*-Cp*W(NO)(C_6H_5)(H)(PMe_3) formed by the C−H bond activation of C_6H_6 by *trans*-Cp*W(NO)(CH_2SiMe_3)(H)(PMe_3) originates with the benzene substrate. Second, *cis*-Cp*W(NO)(C_6H_5)(H)(PMe_3) slowly converts to *cis*-Cp*W(NO)(C_6D_5)(D)(PMe_3) when left in C_6D_6 for 6 days under ambient conditions, thereby indicating the kinetic lability of the reactant and the thermodynamic stability of the product under these experimental conditions. Finally, the syntheses of *cis*-Cp*W(NO)(C_6H_5)(H)(PMe_3) and *cis*-Cp*W(NO)(C_6D_5)(D)(PMe_3) can be successfully effected from both *trans*-

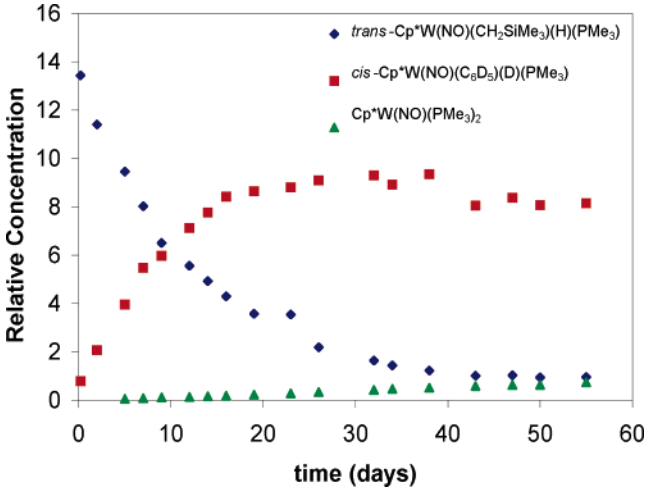

Figure 3. Relative concentrations of the reactant and products versus time in a C_6D_6 solution of *trans*-Cp*W(NO)(CH_2SiMe_3)(H)(PMe_3), as determined by ^1H NMR spectroscopic monitoring.

Cp*W(NO)(CH_2SiMe_3)(H)(PMe_3) and *trans*-Cp*W(NO)(CH_2CMe_3)(H)(PMe_3) reactants.

Kinetic Studies of the Benzene C−H Activation Processes. The C−H bond activations of neat C_6H_6 and C_6D_6 by *trans*-Cp*W(NO)(CH_2SiMe_3)(H)(PMe_3) and *trans*-Cp*W(NO)(CH_2CMe_3)(H)(PMe_3) have been monitored by ^1H or $^{31}P\{^1H\}$ NMR spectroscopy at 20 °C for more than 3 half-lives (Figure 3). Measurements of the kinetics at different temperatures in order to obtain kinetic parameters such as the enthalpies and entropies of activation have not been attempted, since the extent of formation of side products varies unpredictably with temperature. All investigated reactions display pseudo-first-order kinetics for the consumption of the starting organometallic complex. The half-life for the loss of *trans*-Cp*W(NO)(CH_2SiMe_3)(H)(PMe_3) is 10.0 ± 0.2 days when monitored by ^1H NMR spectroscopy, and the rate of disappearance of the starting organometallic complex is not affected by the presence of 1 equiv of PMe_3 or by varying the substrates (i.e. either C_6H_6 or C_6D_6). The formation of either product, *cis*-Cp*W(NO)(C_6H_5)(H)(PMe_3) or *cis*-Cp*W(NO)(C_6D_5)(D)(PMe_3), is not sufficiently clean to permit any conclusion to be drawn as to the kinetic order of their formation. Side products such as Cp*W(NO)(PMe_3)$_2$ are formed both directly from the reactant and from the main products, thereby complicating these kinetic studies.

As shown by ^1H NMR spectroscopy, thermolysis of *trans*-Cp*W(NO)(CH_2SiMe_3)(D)(PMe_3) in C_6D_6 at 20 °C results in a pseudo-first-order loss of the reactant with a half-life of 10.9 ± 0.2 days, as compared to 10.0 ± 0.2 days for *trans*-Cp*W(NO)(CH_2SiMe_3)(H)(PMe_3). The kinetic isotope effect (KIE), k_H/k_D, is a very small 1.1 and is probably not very meaningful in light of the experimental errors associated with these measurements.

The experimental studies are consistent with the probable mechanism summarized in Scheme 2, in which R = CH_2CMe_3, CH_2SiMe_3 and R′ = C_6H_5. This mechanism involves initial formation of a σ-alkane complex from *trans*-Cp*W(NO)(R)(H)(PMe_3) (R = CH_2CMe_3, CH_2SiMe_3), followed by the intramolecular reductive elimination of the alkane to form the 16-electron reactive intermediate Cp*W(NO)(PMe_3). A new hydrocarbon substrate such as benzene then coordinates to this intermediate either by donation of its C−H σ-bond electron density to the metal center (as shown in Scheme 2) or by donation of its C−C π-bond electron density. In any event, the hydrocarbon then oxidatively adds to the tungsten center to form the final complex, *cis*-Cp*W(NO)(C_6H_5)(H)(PMe_3).

Scheme 2

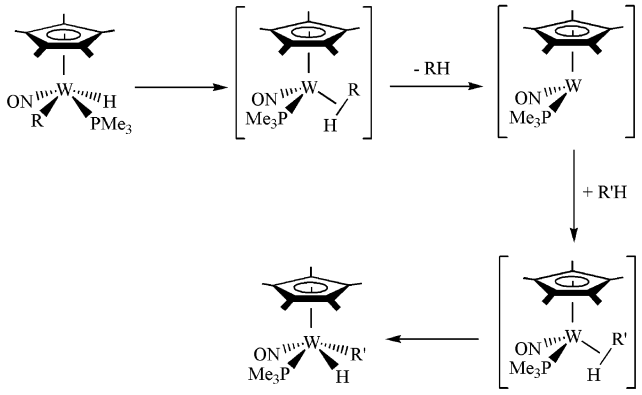

Theoretical Investigations into C−H Activations by CpW(NO)(R)(H)(PMe_3) Complexes. The structures and relative energies of the complexes and transition states have been optimized by DFT calculations. The preliminary examination of the CpW(NO)(R)(H)(PMe_3) systems at the B3LYP/LanL2DZ and the more extended B3LYP/SDD + 6-31G(d,p) + 6-31G levels (see Experimental Section) has revealed that the use of larger basis sets significantly affects both the geometries and energies of the complexes. This feature contrasts with the case for the previously investigated CpM(NO)(R)(R′) systems,[7−9] for which the use of larger basis sets only slightly affects the calculated structures and energies. This dependence on the basis set employed is probably caused by the inclusion of d orbitals for P atoms in the 6-31G(d,p) basis set (very important for generation of the hypervalent character of P atoms), while no d orbitals are assigned to P atoms in the LanL2DZ basis set. Consequently, the larger basis set SDD + 6-31G(d,p) + 6-31G was used in the following calculations. Figure 4 and Table 1 show the reaction paths for the transformations of *trans*-CpW(NO)(R)(H)(PMe_3) (R = methyl (CH_3), neopentyl (CH_2CMe_3)) complexes into *cis*- or *trans*-CpW(NO)(C_6H_5)(H)(PMe_3) complexes and their electronic plus zero-point energies relative to that of the common intermediate CpW(NO)(PMe_3) (**G**). The optimized structures are collected in Figure 5, and their selected bond distances and angles are listed in Table 2.

The metrical parameters of the theoretically optimized structure of *cis*-CpW(NO)(C_6H_5)(H)(PMe_3) (**L**) and the X-ray structure of *cis*-Cp*W(NO)(C_6D_5)(D)(PMe_3) (Figure 1) may be compared. The Cp−W, W−NO, and W−phenyl dimensions are generally comparable in both structures. For example, the computed distances of

(7) (a) Adams, C. S.; Legzdins, P.; McNeil, W. S. *Organometallics* **2001**, *20*, 4939. (b) Adams, C. S.; Legzdins, P.; Tran, E. *Organometallics* **2002**, *21*, 1474. (c) Wada, K.; Pamplin, C. B.; Legzdins, P.; Patrick, B. O.; Tsyba, I.; Bau, R. *J. Am. Chem. Soc.* **2003**, *125*, 7035.
(8) Poli, R.; Smith, K. M. *Organometallics* **2000**, *19*, 2858.
(9) Fan, Y.; Hall, M. B. *Dalton* **2002**, 713.

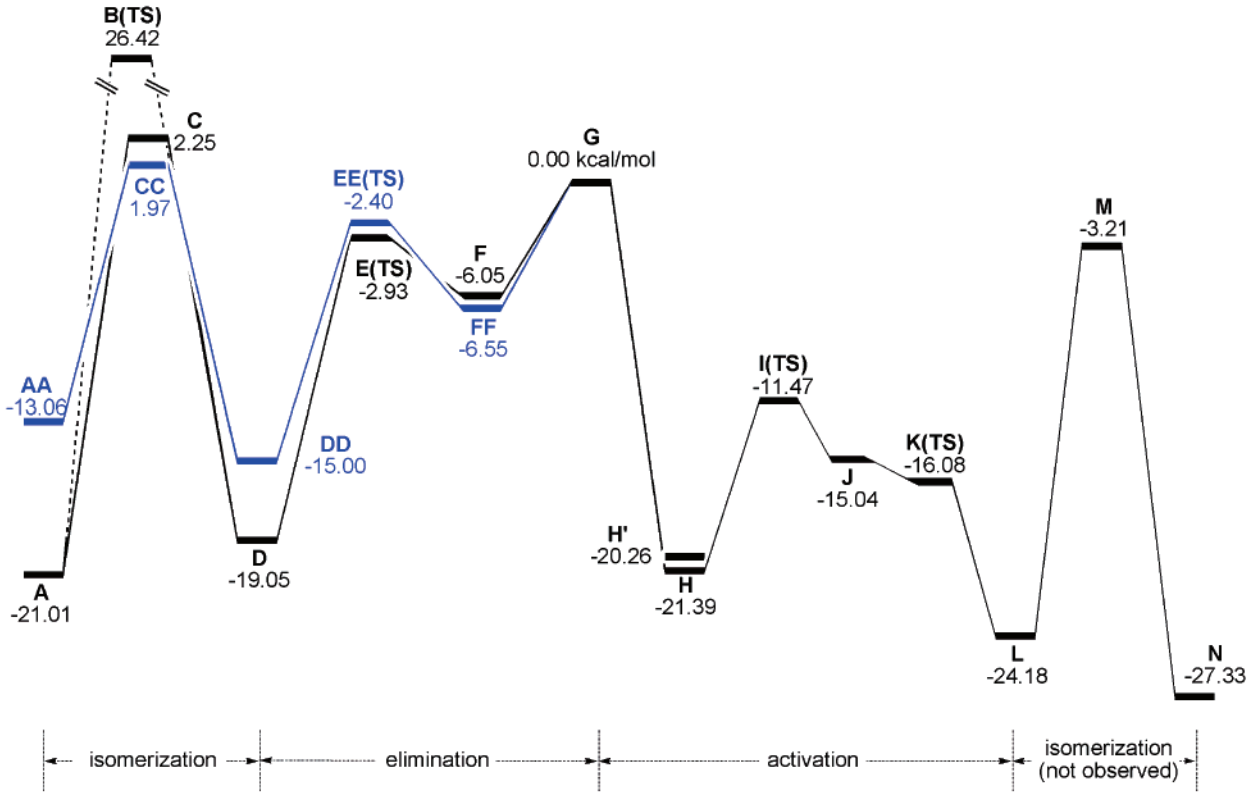

Figure 4. E_0 profile of CpW(NO)(PMe_3) complexes derived from **A** and **AA**.

Table 1. Energies (kcal mol^{-1}) of the Optimized Structures and the Transition States[a]

	A	AA	B	C	CC	D	DD	E	EE	F	FF	G	H	H′	I	J	K	L	M	N
ΔE_0	−21.01	−13.06	26.42	2.25	1.97	−19.05	−15.00	−2.93	−2.40	−6.05	−6.55	0.00	−21.39	−20.26	−11.47	−15.04	−16.08	−24.18	−3.21	−27.33
ΔE	−21.51	−12.68	26.05	1.40	1.80	−19.40	−14.51	−3.17	−1.95	−5.67	−5.58	0.00	−20.82	−19.70	−10.91	−14.13	−15.63	−23.36	−3.03	−26.62
ΔH	−22.11	−13.28	25.46	1.40	1.80	−19.99	−15.10	−3.76	−2.54	−6.26	−6.17	0.00	−21.41	−20.29	−11.50	−14.73	−16.22	−23.95	−3.03	−27.21
ΔG	−10.02	0.23	37.41	0.62	2.03	−7.89	−1.90	7.48	10.34	3.77	4.49	0.00	−8.00	−6.38	1.33	−3.13	−3.05	−11.67	−3.61	−14.60

[a] Definitions: ΔE_0, electronic and zero-point energies; ΔE, electronic and thermal energies; ΔH, electronic and thermal enthalpies; ΔG, electronic and thermal free energies.

W−N = 1.799 Å, N−O = 1.207 Å, and W−C1 = 2.224 Å are very similar to those found in the X-ray structure (i.e. W−N = 1.7831(15) Å, N−O = 1.222(2) Å, and W−C11 = 2.1968(19) Å, respectively). The distances between the W and P atoms are also comparable (i.e. 2.477 Å in the calculation and 2.4557(5) Å in the X-ray structure), thereby indicating that the calculations at the present level satisfactorily reproduce the molecular structure of the complex. Only the optimized W−H value of 1.737 Å is significantly longer than the found W−D distance of 1.51(3) Å.

The reaction pathways from *trans*-CpW(NO)(R)(H)(PMe_3) (R = CH_3 (**A**), CH_2CMe_3 (**AA**)) to their *cis*-R,H isomers have been investigated. The *trans*-CH_3,H complex **A** is thermodynamically more stable than its *cis*-CH_3,H isomer **D** by 1.96 kcal mol^{-1}. On the other hand, the *trans*-CpW(NO)(CH_2CMe_3)(H)(PMe_3) complex **AA** is less stable than its *cis*-CH_2CMe_3,H isomer **DD**, thereby indicating that *trans*-CpW(NO)(CH_2CMe_3)(H)(PMe_3) is a kinetic product. The calculated P−W−C1 bond angle found in **AA** is 81.6°, significantly larger than in the simplified complex **A** (76.5°), thus indicating that steric repulsion between the bulky neopentyl group and the PMe_3 ligand significantly distorts and destabilizes the trans isomer **AA**. Consequently, as was found for the Cp′Mo(NO)($R)_2$ systems,[7−9] the results obtained in these systems by using simplified models such as CpW(NO)(CH_3)(H)(PMe_3) in place of the actual and more complicated complexes should be interpreted with caution.[7c]

There are two possible pathways for the transformation from **A** (or **AA**) to **D** (or **DD**). One is the direct isomerization from *trans*-R,H to *cis*-R,H isomers. Similar direct isomerization from *trans*-CpRe(CO)$_2$(R)(H) to its cis isomer has been examined theoretically by Clot et al., and it has been found to be the rate-determining step of the C−H bond activation process.[10] After extensive investigation, we have optimized a suitable transition state (**B(TS)**) of this direct pathway. The IRC calculation clearly suggests that **B(TS)** is a true transition state from **A**. The transition state can be described as having a piano-stool structure, with the transferring hydrido ligand (H*) being located below the W atom but shifted slightly toward the P atom. The calculated bond distance between W and H* is 1.854 Å, slightly longer than those found in **A** and **D**. However, its energy level relative to **A** is very high at 47.43 kcal mol^{-1}. Therefore, the direct pathway via **B(TS)** is expected to occur hardly at all at just above room temperature.

Another possible pathway from the trans to the cis isomers is via dissociation and recoordination of the PMe_3 ligand. As shown in Figure 4 and Table 1, the

(10) Clot, E.; Oelckers, B.; Klahn, A. H.; Eisenstein, O.; Perutz, R. N. *Dalton* **2003**, 4065.

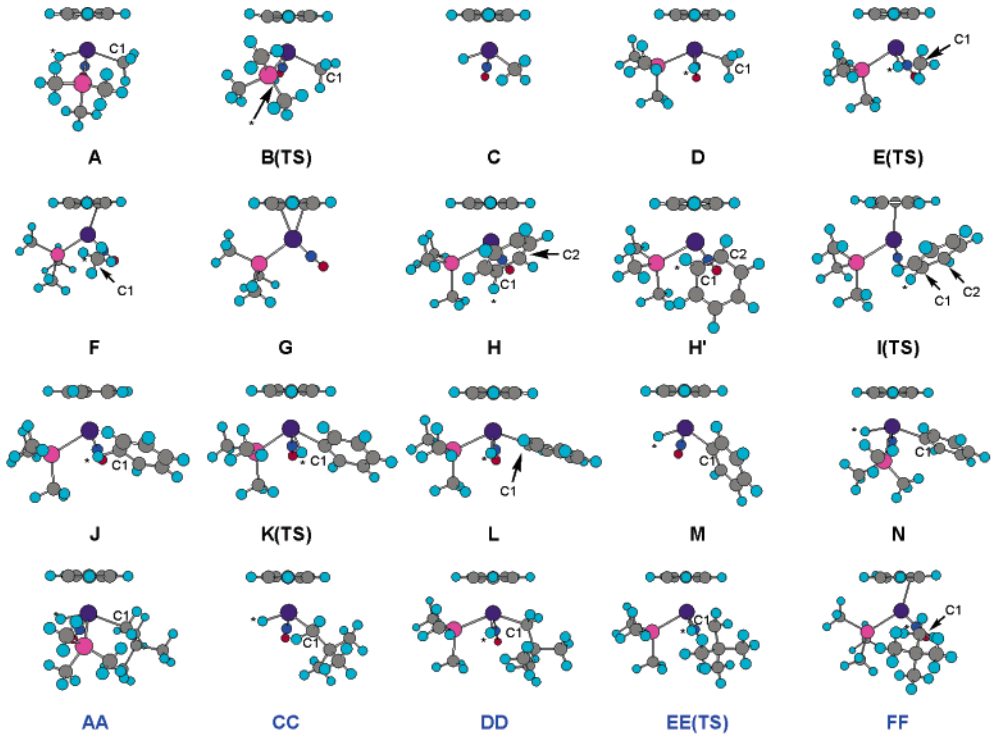

Figure 5. Optimized structures of CpW(NO)(PMe_3) complexes derived from **A** and **AA**.

Table 2. Selected Bond Distances and Angles of the Optimized Structures and the Transition States

	A	AA	B	C	CC	D	DD	E	EE	F	FF	G	H	H′	I	J	K	L	M	N
									Bond Distances (A)											
W−N	1.797	1.794	1.868	1.791	1.790	1.799	1.798	1.807	1.801	1.807	1.804	1.805	1.796	1.797	1.805	1.805	1.802	1.799	1.789	1.796
N−O	1.204	1.206	1.224	1.199	1.202	1.208	1.210	1.210	1.212	1.212	1.213	1.210	1.212	1.209	1.215	1.210	1.209	1.207	1.201	1.206
W−P	2.538	2.546	2.462			2.476	2.470	2.420	2.432	2.427	2.431	2.442	2.470	2.468	2.428	2.431	2.438	2.477		2.538
W−C1	2.261	2.307	2.240	2.118	2.097	2.242	2.271	2.407	2.406	2.768	2.788		2.346	2.362	2.636	2.338	2.276	2.224	2.128	2.237
W−C2													2.296	2.228	3.116					
W−H*	1.726	1.725	1.854	1.722	1.722	1.743	1.732	1.767	1.758	2.051	2.064		2.865	2.848	2.500	1.862	1.793	1.737	1.717	1.725
C1−H*	3.762	3.814	3.008	3.188	3.128	2.279	2.306	1.379	1.434	1.134	1.140		1.087	1.090	1.093	1.219	1.344	2.266	3.192	3.721
C1−C2													1.464	1.458	1.406					
									Bond Angles (deg)											
W−N−O	173.6	172.1	171.4	173.4	172.3	175.4	173.4	175.9	175.7	176.4	176.3	175.1	173.8	174.9	176.0	173.4	173.8	174.1	172.9	171.9
P−W−N	98.2	99.7	109.6			86.3	86.8	89.0	89.8	88.9	89.6	90.9	88.1	88.5	89.7	90.6	89.9	86.0		92.2
P−W−C1	76.5	81.6	87.0			130.1	131.2	107.5	112.8	97.4	104.7		81.4	82.2	94.1	105.9	108.6	130.1		59.3
P−W−C2													117.6	117.7	120.1					
C1−W−N	90.2	94.2	99.2	96.8	100.3	88.9	91.6	91.9	92.8	92.5	93.2		97.8	103.3	96.5	94.6	94.1	90.9	97.2	95.2
C1−W−H*	90.0	141.7	94.1	111.8	109.6	68.5	68.8	34.5	36.2	21.2	21.1		21.2	21.7	24.4	31.2	36.2	68.5	111.8	139.4
C2−W−N													92.1	95.0	90.4					

barriers for the dissociation of PMe_3 from **A** or **AA** are moderate. As before, the energy barrier for the neopentyl complex (15.03 kcal mol^{-1}) is significantly lower than that for the methyl complex (23.26 kcal mol^{-1}), again manifesting the significant effect of the size of the alkyl groups. The dissociation of the PMe_3 ligand is entropically favorable, although the exact evaluation of ΔG in solution by DFT calculations is difficult. Nevertheless, it is not unreasonable to expect that these barriers for dissociation of PMe_3 might be readily overcome at just above room temperature. The optimized structures of the intermediates (**C** and **CC**) involve strong agostic interactions[11] between W atoms and α-hydrogens of the alkyl ligands. The W−C1−H* angles are 87.6 and 76.0° in the optimized structures of **C** and **CC**, respectively. These values are significantly smaller than the normal value (109.5°) expected for an sp^3-hybridized C atom. Similar α-agostic interactions have also been found in the Cp′M(NO)R_2 systems (M = Mo, W).[7−9,12] It should be noted at this point that the DFT calculations have excluded the possibility of the coordination of benzene instead of PMe_3 onto these intermediates, **C** and **CC**. For **C** and **CC**, there are also small activation barriers (∼1 kcal/mol) for the coordination of hydrocarbons, which are not shown in the diagram.

The reductive elimination of alkyl and hydrido ligands from the *cis*-R,H intermediates **D** and **DD** proceeds smoothly with moderate activation barriers via the transition states **E(TS)** and **EE(TS)**, to form the corresponding *σ*-alkane complexes **F** and **FF**. The barriers for the reductive eliminations from the methyl and neopentyl complexes have been computed to be 16.12 and 12.60 kcal mol^{-1}, respectively. The transition states are late ones, in which the formation of alkanes is almost complete. The distances between the transferring hydrogen (H*) and the methyl and neopentyl carbons

(11) Crabtree, R. H. *The Organometallic Chemistry of the Transition Metals*, 3rd ed.; Wiley: New York, 2001.

(12) Bau, R.; Mason, S. A.; Patrick, B. O.; Adams, C. S.; Sharp, W. B.; Legzdins, P. *Organometallics* **2001**, *20*, 4492.

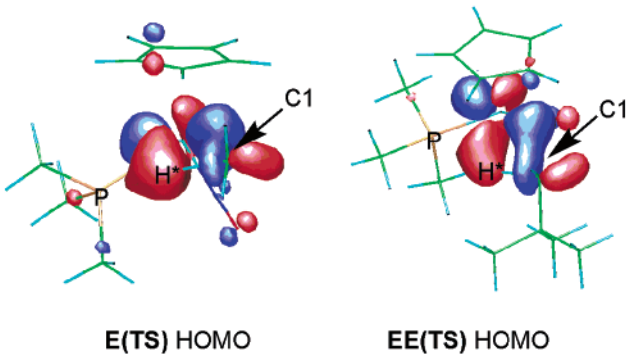

Figure 6. HOMOs of the transition states **E(TS)** and **EE(TS)**.

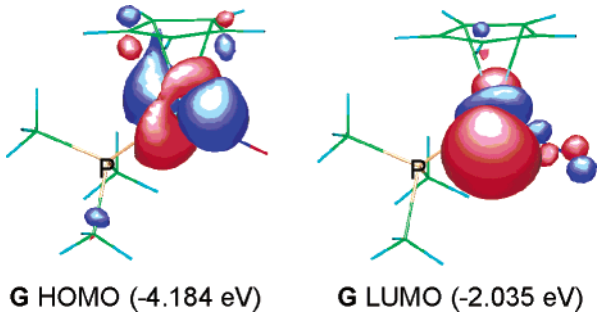

Figure 7. HOMO and LUMO of the intermediate **G**.

are only 1.379 and 1.434 Å, respectively. Figure 6 shows the HOMOs of **E(TS)** and **EE(TS)**, in which back-donation of electrons from a d orbital of the W atom into the C−H antibonding orbital of the alkane can be recognized. Loss of alkanes from σ-alkane complexes requires further energy, but this process is obviously entropically very favored. As shown in Figure 7, this intermediate **G** possesses a high-energy HOMO (the nonbonding t_{2g} d orbital) and a low-lying LUMO (the e_g d orbital), thus indicating that this remarkable complex has both Lewis acidic and Lewis basic character. The Lewis acidic, low-lying LUMO promotes the coordination of alkanes or arenes, while the HOMO electrons are donated to a π^* orbital of coordinating arenes or a σ^* orbital of alkanes. In addition, the direction of the HOMO of **G** is very suitable for back-bonding to the coordinating C−H or C−C bonds.

The coordination of benzene to **G** greatly reduces the potential energy. Two adducts can be optimized, but **H** is more stable. For both complexes, the C−H bonds on the two coordinating carbons of benzene are found to be bent away from the W atom. The bond distances (C1−C2) in **H** and **H′** are increased to 1.464 and 1.458 Å, respectively, thereby reflecting the contribution of metallacyclopropane character caused by the significant back-donation of electrons from a W filled d orbital to the empty π^* orbital of benzene.

The σ-like benzene complex **J** has been successfully located by the use of the large basis set. Again, the coordinating C−H bond is significantly bent and the C1−H* bond distance is relatively long at 1.219 Å. The transition state between the π- and σ-coordinated benzene complexes **I(TS)** has also been successfully located. The IRC study confirms that **I(TS)** is a true TS. The energy required to overcome this barrier from **H** is 9.92 kcal mol^{-1}, which is less than that required

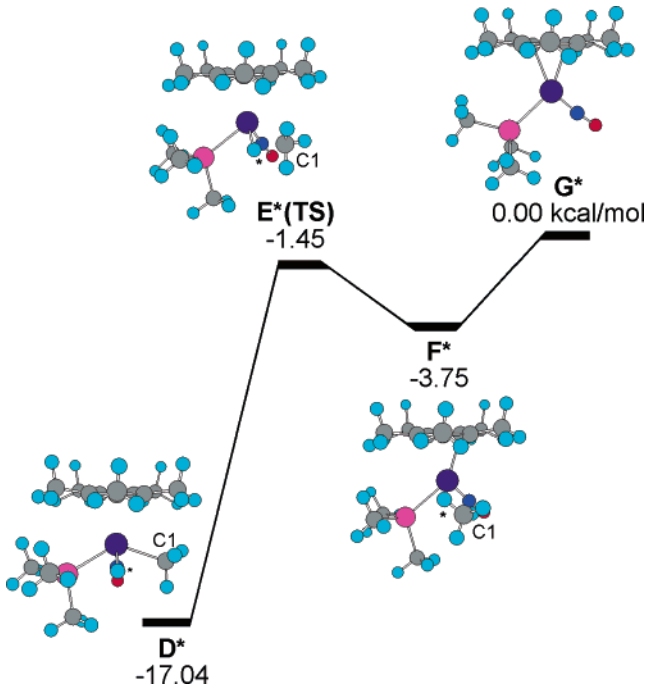

Figure 8. E_0 profile of the reductive elimination process starting from *cis*-Cp*W(NO)(CH_3)(H)(PMe_3).

Table 3. Energies (kcal mol^{-1}) of the Optimized Structures and the Transition States

	D*	E*	F*	G*
ΔE_0	−17.04	−1.45	−3.75	0.00
ΔE	−17.45	−1.76	−3.35	0.00
ΔH	−18.04	−2.35	−3.94	0.00
ΔG	−6.07	9.34	6.14	0.00

for the reductive elimination of alkanes from the intermediates **D** and **DD**. From the intermediate **J**, the cleavage of the coordinated C−H bond proceeds without a significant energetic barrier. In terms of electronic energies the located transition state **K(TS)** is slightly less stable than **J**, but on the basis of E_0 **J** is less stable than **K(TS)**. The IRC study also establishes that **K(TS)** is the transition state between **J** and the final product **L**. **K(TS)** is an early transition state, and so there are only slight differences between the molecular geometries of **J** and **K(TS)**. Experimentally, the final product is *cis*-Cp*W(NO)(C_6H_5)(H)(PMe_3), and there is no evidence for the formation of the trans isomer. The DFT calculations show that *trans*-CpW(NO)(C_6H_5)(H)(PMe_3) (**N**) is thermodynamically more stable than its cis isomer **L**. However, there is a large E_0 barrier (20.97 kcal mol^{-1}) for the dissociation of a PMe_3 ligand from the cis complex, which would hamper further isomerization of the cis complex to its trans isomer at moderate temperatures. Again, there are small additional activation barriers (~2 kcal/mol) for the coordination of hydrocarbons to the intermediate **M**.

The effect of the methyl groups on the cyclopentadienyl ligand has also been examined. Figure 8 shows the E_0 diagram for the reductive-elimination pathway from *cis*-Cp*W(NO)(CH_3)(H)(PMe_3) (**D***) to the formally 16-electron intermediate (**G***), and Tables 3 and 4 contain their relative energies and selected geometrical parameters. The presence of five electron-donating methyl groups on the Cp* ring increases the electron density of the tungsten center. The σ-methane complex **F*** is

Table 4. Selected Bond Distances and Angles of the Optimized Structures and the Transition States

	D*	E*	F*	G*
	Bond Distances (Å)			
W−N	1.799	1.802	1.804	1.806
N−O	1.213	1.215	1.215	1.214
W−P	2.485	2.436	2.464	2.462
W−C1	2.242	2.409	2.792	
W−H*	1.750	1.770	2.596	
C1−H*	2.276	1.386	1.095	
	Bond Angles (deg)			
W−N−O	174.8	174.8	174.5	173.7
P−W−N	84.5	88.7	89.3	89.8
P−W−C1	126.0	105.3	86.7	
C1−W−N	87.4	92.1	99.3	
C1−W−H*	68.2	34.7	23.1	

more stable than **G***, but only by 3.75 kcal mol^{-1}, while the relative energy of **F** versus **G** is −6.05 kcal mol^{-1}. This difference is probably due to the lower Lewis acidity of the 16-electron intermediate (**G***) as compared with its Cp analogue (**G**). Steric repulsion between the incoming methane and the methyl groups on the Cp* ring also seems to be possible in **F***. The presence of the Cp* ligand also destabilizes the hydrido methyl complex **D***. Therefore, the barrier for the reductive elimination process starting from **D*** (15.59 kcal mol^{-1}) is significantly lower than that for the CpW(NO)(CH_3)(H)(PMe_3) system. The molecular geometries of the Cp* complexes are very similar to those of the Cp complexes. For example, the bond distances of **D** and **D*** shown in the tables differ by less than 0.01 Å. The P−W−C1 angle is slightly more acute in **D*** than in **D**, probably because of the steric effect of the bulky Cp* ligand.

On the basis of the total energy diagram, the rate-determining step can be either the isomerization of the trans reactants to their cis forms or the loss of alkanes from the *cis*-Cp*W(NO)(R)(H)(PMe_3) complexes, since both have similar barriers. The experimental study of the *trans*-Cp*W(NO)(CH_2SiMe_3)(H)(PMe_3) system indicates that addition of 1 equiv of PMe_3 does not affect the reaction rate, thus suggesting that isomerization via dissociation and recoordination of a PMe_3 ligand is not the rate-determining pathway. However, the resulting *cis*-Cp*W(NO)(CH_2SiMe_3)(H)(PMe_3) is not detectable by ^{1}H NMR spectroscopic monitoring (Figure 3). The E_0 diagram in Figure 4 also shows that the barriers for the reductive elimination from the alkyl hydrido complexes **D** and **DD** are greater than that for the formation of the σ-arene complex **J** from the π-arene complex **H**. Obviously, the loss of alkane from the σ-alkane complex is favorable, considering the increase in entropy. The experimentally determined KIE is small and therefore consistent with the reductive-elimination process being rate determining, since small or inverse KIEs have been found for similar processes,[13] but it is probably not meaningful. Unfortunately, the reaction kinetics are not very clean, and so a definitive answer concerning the rate-determining steps of these transformations cannot be provided at the present time.

The present DFT study also reveals that the additional two electrons supplied by the PMe_3 ligand to W change the C−H activation mechanism. For the formally 16-electron Cp′W(NO)(R)(R′) systems, a σ-bond

(13) Jones, W. D. *Acc. Chem. Res.* **2003**, *36*, 140.

Scheme 3

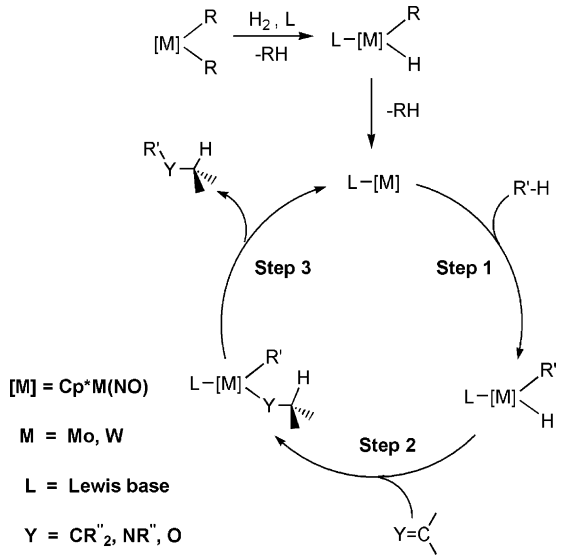

metathesis-like mechanism has been invoked previously. In their theoretical study of mechanisms for generating tungsten carbene species from Cp′W(NO)(CH_3)$_2$ (Cp′ = Cp, Cp*), Fan and Hall[9] have found a stable intermediate corresponding to α-H oxidative addition, namely Cp′W(NO)(H)(=CH_2)(CH_3). However, they suggest that a one-step, σ-bond metathesis-like mechanism is preferred. In contrast, in the present study reductive-elimination/oxidative-addition processes govern the C−H bond activation reactions. The additional two electrons make the metal center more electron-rich and thus more prone to undergo oxidative-addition processes. If σ-bond metathesis processes were operative, the conversions would proceed via Cp*W(NO)(PMe_3)(alkylidene)-type species as reactive intermediates, and we have previously shown that such 18-electron complexes do not activate C−H bonds under ambient conditions.[3] Finally, as discussed in the preceding paragraphs, the spatial orientations of the HOMOs in these complexes are also suitable for the reductive elimination/oxidative addition of the C−H bonds of small hydrocarbons.

Epilogue

The single C−H activation processes described in this report are the requisite first steps in the development of these organometallic nitrosyl complexes as catalysts for the selective functionalization of hydrocarbons. In particular, this chemistry suggests to us that specific members of the general family of complexes Cp*M(NO)(R)(H)(L) (M = Mo, W; R = alkyl, aryl; L = Lewis base) may well be capable of functioning as homogeneous catalysts for organic coupling reactions of the type depicted in Scheme 3. We have now demonstrated the three individual steps shown, namely (1) C−H bond activation by oxidative addition of R′−H to M (this work), (2) insertion of C=Y (in which Y is more electronegative than C) into the M−H linkage,[14] and (3) reductive elimination of R′−Y−C−H for particular

(14) Debad, J. D.; Legzdins, P.; Lumb, S. A.; Batchelor, R. J.; Einstein, F. W. B. *Organometallics* **1995**, *14*, 2543.

complexes.[15] The challenge remains to discover complexes that effect all three steps, and research specifically directed toward that objective is currently in progress.

Experimental Section

General Methods. All reactions and subsequent manipulations were performed under rigorously anaerobic and anhydrous conditions utilizing either high vacuum or an atmosphere of prepurified argon or dinitrogen with conventional glovebox and vacuum-line Schlenk techniques. The gloveboxes used were Innovative Technologies LabMaster 100 and MS-130 BG dual-station models equipped with freezers maintained at −30 °C. Thermolysis reactions were performed in thick-walled glass pressure vessels equipped with Kontes greaseless stopcocks, and NMR spectroscopic analyses were conducted in J. Young NMR tubes.

All solvents were dried and distilled prior to use or vacuum-transferred directly from the appropriate drying agent. Hydrocarbons and diethyl ether were distilled from sodium benzophenone ketyl, tetrahydrofuran was distilled from molten potassium, and dichloromethane and chloroform were distilled from calcium hydride. Deuterated solvents were purchased from Cambridge Isotope Laboratories and then degassed and vacuum-transferred from K (C_6D_6), Na (toluene-d_8), or activated 4 Å molecular sieves (CD_2Cl_2). Trimethylphosphine (Aldrich) was dried and stored over potassium. Celite and neutral alumina I (60−325 mesh) were oven-dried and cooled under vacuum prior to use. Cp*W(NO)$(CH_2SiMe_3)_2$[16] and Cp*W(NO)$(CH_2CMe_3)_2$[12] were prepared according to literature procedures; all other reagents were purchased from commercial suppliers and were used as received.

Infrared spectra were recorded on an ATI Mattson Genesis Series FT-IR spectrometer. NMR spectra were recorded at room temperature, unless otherwise noted, on Bruker AV300 and AMX 500 spectrometers. ^{1}H and ^{13}C chemical shifts are recorded in ppm relative to the residual proton or natural-abundance carbon signal(s) of the solvents employed; coupling constants are reported in Hz. ^{2}H{^{1}H} NMR signals were referenced to C_6H_5D (δ 7.15). Correlation and assignment of ^{1}H and ^{13}C NMR resonances were aided by 2D HMQC and HMBC experiments when necessary. Low-resolution mass spectra (EI, 70 eV) were recorded by the staff of the UBC mass spectrometry facility using a Kratos MS-50 spectrometer. Elemental analyses were performed by Mr. Minaz Lakha of the UBC microanalytical facility.

Preparation of *trans*-Cp*W(NO)$(CH_2SiMe_3)(H)(PMe_3)$. This complex was synthesized by a modification of the previously reported method.[5] Cp*W(NO)$(CH_2SiMe_3)_2$ (0.491 g, 0.939 mmol) was dissolved in hexanes (10 mL) in a 100 mL Teflon-sealed pressure vessel, and then a hexanes solution of PMe_3 (6.48 mL, 0.217 M, 1.5 equiv) was added to the vessel via syringe under a flow of Ar. The Ar atmosphere was next removed under vacuum, and the Teflon-sealed vessel was refilled with H_2 (ca. 1 atm). The original purple solution became brownish yellow after being stirred for 20 h, after which time the volatile components of the reaction mixture were removed in vacuo. The dried residue was dissolved in 2:1 ether/hexanes, and the solution was filtered through a column (1 × 2 cm) of Celite supported on a medium-porosity glass frit. The volume of the filtrate was reduced in vacuo, and the concentrated solution was maintained at −33 °C for 2 days to induce the deposition of dark brown crystals of *trans*-Cp*W(NO)$(CH_2SiMe_3)(H)(PMe_3)$ (0.26 g, 54% yield).

IR (Nujol): 1853 (w, ν_{W-H}), 1546 (s, ν_{NO}) cm^{-1}. MS (EI): *m/z* 513 (P^+). ^{1}H NMR (500 MHz, C_6D_6): δ −1.26 (ddd, 1H, $^1J_{HW}$ = 56.6 Hz, $^2J_{HP}$ = 88.2 Hz, WH_W), −0.68 (ddd, 1H, $^2J_{HH}$ = 13.6 Hz, $^3J_{HP}$ = 16.8 Hz, $^3J_{HH}$ = 5.9 Hz, WCH_AH$_B$), −0.97 (ddd, 1H, $^2J_{HH}$ = 13.6 Hz, $^3J_{HP}$ = 16.8 Hz, $^3J_{HH}$ = 5.9 Hz, WCH$_A$$H_B$), 0.49 (s, 9H, CH_2Si*Me*$_3$), 1.09 (d, 9H, $^2J_{PH}$ = 8.3 Hz, P*Me*$_3$), 1.78 (s, 15H, C_5*Me*$_5$). ^{31}P{^{1}H} NMR (300 MHz, C_6D_6): δ −27.4 (s, $^1J_{PW}$ = 194 Hz). ^{13}C{^{1}H} NMR (75.48 MHz, C_6D_6): δ −5.3 (d, $^2J_{CP}$ = 13.6 Hz, *C*H$_2$SiMe$_3$), 4.4 (s, CH_2Si*Me*$_3$), 11.2 (s, C_5*Me*$_5$), 19.3 (d, $^1J_{CP}$ = 30.2 Hz, P*Me*$_3$), 105.4 (s, *C*$_5$Me$_5$). ^{1}H-selective NOE (400 MHz, C_6D_6): irrad at δ −1.25, NOE at 1.09; irrad at −0.97, NOE at −0.68; irrad at −0.68, NOE at −0.97; and 1.09; irrad at 0.49, NOE at 1.09; irrad at 1.09, NOE at −1.25 and −0.68. Anal. Calcd for $C_{17}H_{36}$NOPW: C, 39.77; H, 7.07; N, 2.73. Found: C, 39.90; H, 6.84; N, 2.94.

Preparation of *cis*-Cp*W(NO)$(CH_2SiMe_3)(H)(PMe_3)$. *trans*-Cp*W(NO)$(CH_2CMe_3)(H)(PMe_3)$ (0.03 g) was dissolved in tetramethylsilane (90 mL) in a 250 mL Teflon-sealed vessel. The yellow solution became brown after being stirred for 22 days, after which time the volatile components of the reaction mixture were removed in vacuo. The dried residue was dissolved in pentane, and the solution was filtered through Celite (0.5 × 2 cm). The filtrate was taken to dryness to obtain a brown residue, which was dissolved in C_6D_6 for ^{1}H-selective NOE spectra.

^{1}H NMR (300 MHz, C_6D_6): δ −1.26 (ddd, 1H, $^1J_{HW}$ = 56.6 Hz, $^3J_{HH}$ = 12.4 Hz, $^2J_{HP}$ = 88.2 Hz, WH_W), −0.68 (ddd, 1H, $^2J_{HH}$ = 13.6 Hz, $^3J_{HP}$ = 16.8 Hz, $^3J_{HH}$ = 5.9 Hz, WCH_AH$_B$), −0.97 (ddd, 1H, $^2J_{HH}$ = 13.6 Hz, $^3J_{HP}$ = 16.8 Hz, $^3J_{HH}$ = 5.9 Hz, WCH$_A$$H_B$), 0.49 (s, 9H, CH_2Si*Me*$_3$), 1.09 (d, 9H, $^2J_{PH}$ = 8.3 Hz, P*Me*$_3$), 1.78 (s, 15H, C_5*Me*$_5$). ^{31}P{^{1}H} NMR (300 MHz, C_6D_6): δ −27.4 (s, $^1J_{PW}$ = 194 Hz). ^{1}H-selective NOE (400 MHz, C_6D_6): irrad at δ −1.24, NOE at −0.96 and −0.67; irrad at −0.96, NOE at −1.24 and −0.67; irrad at −0.67, NOE at −1.24 and −0.96; irrad at 1.10, NOE at 0.49.

Preparation of *trans*-Cp*W(NO)$(CH_2SiMe_3)(D)(PMe_3)$. Cp*W(NO)$(CH_2SiMe_3)_2$ (0.400 g, 0.764 mmol) was dissolved in hexanes (20 mL) in a 100 mL Teflon-sealed pressure vessel, and then PMe_3 (0.6 mL, 8 equiv) was vacuum-transferred into the vessel. The vessel was then evacuated and refilled with D_2. The original purple solution turned brownish red while being stirred for 20 h, after which time the volatile components of the reaction mixture were removed in vacuo. The dried residue was dissolved in 2:1 ether/hexanes (60 mL), and the solution was filtered through Celite (2 × 4 cm) to obtain an orange-yellow eluate. The volume of the eluate was reduced in vacuo, and the concentrated solution was stored at −33 °C for 2 days to induce the deposition of orange-yellow crystals (0.073 g, 15% yield) of *trans*-Cp*W(NO)$(CH_2SiMe_3)(D)(PMe_3)$.

IR (Nujol): 1545 (s, ν_{NO}), 1300 (w, ν_{WD}) cm^{-1}. MS (EI): *m/z* 514 (P^+). ^{1}H NMR (300 MHz, C_6D_6): δ −0.96 (dd, 1H, $^2J_{HP}$ = 16.7 Hz, $^2J_{HH}$ = 13.5 Hz, WCH$_A$$H_B$), −0.67 (dd, 1H, $^2J_{HH}$ = 13.4 Hz, $^3J_{HP}$ = 25.1 Hz, WCH_AH$_B$), 0.49 (s, 9H, CH_2Si*Me*$_3$), 1.09 (d, 9H, $^2J_{PH}$ = 8.3 Hz, P*Me*$_3$), 1.78 (s, 15H, C_5*Me*$_5$). ^{31}P-{^{1}H} NMR (300 MHz, C_6D_6): δ −27.3 (s, $^1J_{PW}$ = 193.2 Hz, $^2J_{DP}$ = 13.4 Hz). ^{13}C{^{1}H} NMR (75.48 MHz, C_6D_6): δ −5.4 (d, $^2J_{CP}$ = 14 Hz, *C*H$_2$SiMe$_3$), 4.4 (s, $^1J_{CSi}$ = 48 Hz, CH_2Si*Me*$_3$), 11.2 (s, C_5*Me*$_5$), 19.3 (d, $^1J_{CP}$ = 30 Hz, P*Me*$_3$), 105.4 (s, *C*$_5$Me$_5$). Anal. Calcd for $C_{17}H_{35}$DNOPW: C, 39.70; H, 6.80; N, 2.72. Found: C, 39.89; H, 7.10; N, 3.10.

Preparation of *trans*-Cp*W(NO)$(CH_2CMe_3)(H)(PMe_3)$. Cp*W(NO)$(CH_2CMe_3)_2$ (0.404 g, 0.821 mmol) was dissolved in hexanes (50 mL) in a 100 mL Teflon-sealed pressure vessel, and then a hexanes solution of PMe_3 (5.66 mL, 0.217 M,1.5 equiv) was added to the vessel via syringe under a flow of Ar. The atmosphere in the Teflon-sealed vessel was evacuated and then replaced with H_2. The initial wine red solution became orange after being stirred for 20 h, after which time the volatile components of the reaction mixture were removed in vacuo. The dried residue was dissolved in pentane, and the solution was filtered through Celite (1 × 2 cm). The volume of the

(15) Dryden, N. H.; Legzdins, P.; Rettig, S. J.; Veltheer, J. E. *Organometallics* **1992**, *11*, 2583.
(16) Legzdins, P.; Rettig, S. J.; Sánchez, L. *Organometallics* **1988**, *7*, 2394.

filtrate was reduced in vacuo, and the concentrated solution was stored at −33 °C for 2 days to induce the deposition of orange-yellow rectangular prisms of *trans*-Cp*W(NO)(CH_2-CMe_3)(H)(PMe_3) (0.19 g, 47% yield).

IR (Nujol) 1851 (w, ν_{W-H}), 1543 (s, ν_{NO}) cm^{-1}. MS (EI): *m/z* 497 (P^+). ^1H NMR (500 MHz, C_6D_6): δ −1.60 (ddd, 1H, $^1J_{HW}$ = 54.4 Hz, $^3J_{HH}$ = 12.8 Hz, $^2J_{HP}$ = 88.6 Hz, $^3J_{HH}$ = 13.1 Hz, W*H*), 0.69 (ddd, 1H, $^2J_{HH}$ = 13.7 Hz, $^3J_{HP}$ = 22.03 Hz, $^3J_{HH}$ = 5.2 Hz, WCH_AH_B), 1.15 (d, 9H, $^2J_{PH}$ = 8.13 Hz, P*Me*$_3$), 1.44 (s, 9H, CH_2C*Me*$_3$), 1.80 (s, 15H, C_5*Me*$_5$), obscured by signals due to the PMe_3 ligand, confirmed by HMQC (WCH_AH_B). $^{31}P\{^1H\}$ NMR (300 MHz, C_6D_6): δ −27.9 (s, $^1J_{PW}$ = 200.5 Hz). $^{13}C\{^1H\}$ NMR (75.48 MHz, C_6D_6): δ 11.2 (s, C_5*Me*$_5$), 19.6 (d, $^1J_{CP}$ = 30.2 Hz, P*Me*$_3$), 31.2 (d, $^2J_{CP}$ = 14.6 Hz, *C*H_2CMe$_3$), 35.6 (s, CH_2C*Me*$_3$), 38.4 (s, CH_2*C*Me$_3$), 105.2 (s, *C*$_5$Me$_5$). ^1H-selective NOE (400 MHz, C_6D_6): irrad at δ −1.63, NOE at 1.12; irrad at 0.69, NOE at 1.12; irrad at 1.12, NOE at −1.63 and 0.69; irrad at 1.45, NOE at 0.69 and 1.12. Anal. Calcd for $C_{18}H_{36}$NOPW: C, 43.47; H, 7.30; N, 2.82. Found: C, 43.82; H, 7.36; N, 3.06.

Preparation of *trans*-Cp*W(NO)(CH_2CMe_3)(D)(PMe_3). Cp*W(NO)(CH_2CMe_3)$_2$ (0.261 g, 0.531 mmol) was dissolved in hexanes (50 mL) in a 100 mL Teflon-sealed pressure vessel, and then a hexanes solution of PMe_3 (3.7 mL, 0.217 M, 1.5 equiv) was added to the vessel via syringe under a flow of Ar. The Teflon-sealed vessel was evacuated and then refilled with D_2. The initial wine red solution turned orange after being stirred for 48 h, after which time the volatile components of the reaction mixture were removed in vacuo. The dried residue was dissolved in pentane, and the solution was filtered through Celite (1 × 2 cm). The volume of the filtrate was reduced in vacuo, and the concentrated solution was stored at −33 °C for 2 days to induce the deposition of *trans*-Cp*W(NO)(CH_2CMe_3)-(D)(PMe_3) (0.13 g, 50% yield).

IR (Nujol): 1351 (w, ν_{W-D}), 1540 (s, ν_{NO}) cm^{-1}. IR (hexanes): 1587 (s, ν_{NO}) cm^{-1}. MS (EI): *m/z* 499 (P^+). ^1H NMR (300 MHz, C_6D_6): δ 0.69 (t, 1H, $^2J_{HH}$ = 13.9 Hz, $^3J_{HP}$ = 13.1 Hz, WCH_AH_B), 1.13 (d, 9H, $^2J_{PH}$ = 8.1 Hz, P*Me*$_3$), 1.46 (s, 9H, CH_2C*Me*$_3$), 1.79 (s, 15H, C_5*Me*$_5$), obscured by signals due to the PMe_3 ligand confirmed by HMQC (WCH_AH_B). $^{31}P\{^1H\}$ NMR (300 MHz, C_6D_6): δ −27.8 (t, $^1J_{PW}$ = 120 Hz, $^2J_{DP}$ = 13 Hz). $^{13}C\{^1H\}$ NMR (75.48 MHz, C_6D_6): δ 11.2 (s, C_5*Me*$_5$), 19.6 (d, $^1J_{CP}$ = 30.0 Hz, P*Me*$_3$), 31.2 (d, $^2J_{CP}$ = 14.6 Hz, *C*H_2CMe$_3$), 35.6 (s, CH_2C*Me*$_3$), 38.4 (s, CH_2*C*Me$_3$), 105.2 (s, *C*$_5$Me$_5$). Anal. Calcd for $C_{18}H_{35}$DNOPW: C, 43.39; H, 7.02; N, 2.81. Found: C, 43.77; H, 7.42; N, 3.13.

Preparation of *cis*-Cp*W(NO)(C_6H_5)(H)(PMe_3). This complex was synthesized by a modification of the previously reported method.[5] *trans*-Cp*W(NO)(CH_2SiMe_3)(H)(PMe_3) (0.09 g) was dissolved in C_6H_6 (1 mL) in a J. Young NMR tube into which a sealed capillary containing C_6D_6 was placed in order to monitor the progress of the reaction. The initial yellow solution turned brown while being kept at 27 °C for 24 days, after which time the volatile components of the reaction mixture were removed in vacuo. The dried residue was dissolved in Et_2O (5 mL), and the solution was transferred to the top of a silica column (0.5 × 5 cm) supported on glass wool. Elution of the column with Et_2O (25 mL) afforded a brownish yellow eluate whose volume was reduced to 0.5 mL in vacuo, and hexanes (2 mL) were then added. The resulting solution was stored at −33 °C for 3 h to induce the deposition of *cis*-Cp*W(NO)(C_6H_5)(H)(PMe_3) (0.01 g, 10% yield). (The low yields of the aryl hydride complexes isolated during this work reflect their high solubility in common organic solvents.)

IR (hexanes): 1812 (w, ν_{W-H}), 1550 (s, ν_{NO}) cm^{-1}. MS (EI, *m/z*): 425 ($P - C_6H_6$)$^+$. ^1H NMR (300 MHz, C_6D_6): δ 1.41 (d, $^2J_{PH}$ = 9.3 Hz, 9H, P*Me*$_3$), 1.63 (s, 15H, C_5*Me*$_5$), 5.15 (d, $^2J_{PH}$ = 96.8 Hz, $^1J_{WH}$ = 78.6 Hz, 1H), 7.13 (t, $^1J_{HH}$ = 7.3 Hz, 1H, C_6H_5 (para)), 7.30 (t, $^1J_{HH}$ = 7.5 Hz, 2H, C_6H_5 (meta)), 8.02 (t, $^1J_{HH}$ = 6.5 Hz, 2H, C_6H_5 (ortho)). $^{31}P\{^1H\}$ NMR (300 MHz, C_6D_6): δ −1.8 (s, $^1J_{PW}$ = 202 Hz). $^{13}C\{^1H\}$ NMR (100.6 MHz, C_6D_6): δ 10.7 (s, C_5*Me*$_5$), 19.2 (d, $^1J_{CP}$ = 36.2 Hz, P*Me*$_3$), 107.8 (s, *C*$_5$Me$_5$), 123.5 (s, C_6H_5 (para)), 128.9 (s, C_6H_5 (meta)), 145.1 (s, C_6H_5 (ortho)), 160.7 (s, C_6H_5 (ipso)). Anal. Calcd for $C_{19}H_{30}$NOPW: C, 45.35; H, 6.01; N, 2.78. Found: C, 45.65; H, 6.03; N, 3.00.

Preparation of *cis*-Cp*W(NO)(C_6D_5)(D)(PMe_3). *trans*-Cp*W(NO)(CH_2CMe_3)(H)(PMe_3) (67 mg) was dissolved in C_6D_6 (0.7 mL) in a J. Young NMR tube. The initial yellow solution turned brown while being kept at 20 °C for 45 days, after which time the volatile components of the reaction mixture were removed in vacuo. The dried residue was dissolved in 1:1 hexanes/diethyl ether (5 mL), and the solution was transferred to the top of a silica column (0.5 × 5 cm) supported on glass wool. Elution of the column with 1:1 hexanes/diethyl ether (10 mL) afforded a brown eluate, which was discarded. Further elution with 1:1 hexanes/diethyl ether (20 mL) produced a purple eluate, whose volume was reduced in vacuo. The concentrated solution was stored at −33 °C for 2 days to induce the deposition of clear yellow crystals of *cis*-Cp*W(NO)(C_6D_5)-(D)(PMe_3) (6 mg, 9% yield).

Alternatively, dissolution of *cis*-Cp*W(NO)(C_6H_5)(H)(PMe_3) in C_6D_6 and maintenance of this mixture at ambient temperatures for 6 days resulted in the consumption of *cis*-Cp*W-(NO)(C_6H_5)(H)(PMe_3) and the formation of *cis*-Cp*W(NO)-(C_6D_5)(D)(PMe_3), as confirmed by ^1H NMR and $^{31}P\{^1H\}$ NMR spectroscopic monitoring.

IR (Nujol): 1339 (w, ν_{W-D}), 1559 (s, ν_{NO}) cm^{-1}. MS (EI, *m/z*): 425 ($P - C_6D_6$)$^+$. ^1H NMR (300 MHz, C_6D_6): δ 1.16 (d, 9H, $^2J_{PH}$ = 9.2 Hz, P*Me*$_3$), 1.63 (s, 15H, C_5*Me*$_5$). $^{31}P\{^1H\}$ NMR (300 MHz, C_6D_6): δ −1.6 (t, $^1J_{PW}$ = 202 Hz, $^2J_{PD}$ = 15 Hz). $^{13}C\{^1H\}$ NMR (100.6 MHz, C_6D_6): δ 10.7 (s, C_5*Me*$_5$), 19.1 (d, $^1J_{CP}$ = 36.0 Hz, P*Me*$_3$), 107.8 (s, *C*$_5$Me$_5$), 119.9 (s, C_6D_5 (para)), 128.9 (s, C_6D_5 (meta)), 144.2 (t, $^2J_{CD}$ = 23.5 Hz, C_6D_5 (ortho)), 159.9 (s, C_6D_5 (ipso)). Anal. Calcd for $C_{19}H_{24}D_6$NOPW: C, 44.81; H, 4.70; N, 2.75. Found: C, 45.30; H, 5.98; N, 2.96.

General Purification Procedure for Cp*W(NO)(Z)(X)-(PMe_3) (Z = CH_2SiMe_3, CH_2CMe_3; X = H, D) Complexes. If any of these complexes required further purification, the following procedure could be employed to purify the crystals. The crystals were dissolved in hexanes, and the solution was transferred to the top of a silica column (1 × 7 cm) made up in hexanes and supported on a frit. The column was eluted with 2:1 hexanes/ether to obtain a pale yellow eluate. The volume of the eluate was reduced in vacuo, and the concentrated solution was stored at −33 °C for 1 day to induce the deposition of analytically pure, pale yellow crystals of the complex.

Kinetic Monitoring of the Reactions of *trans*-Cp*W-(NO)(CH_2SiMe_3)(H)(PMe_3) with C_6D_6 and C_6H_6. The samples used for NMR spectroscopic monitoring of these reactions were prepared by utilizing the following procedures. *trans*-Cp*W(NO)(CH_2SiMe_3)(H)(PMe_3) (10.0 mg) was weighed into a vial, and C_6D_6 (0.60 mL) was added via syringe. A flame-sealed capillary containing tris(4-methoxyphenyl)phosphate dissolved in C_6D_6 was placed into a resealable NMR tube, and the *trans*-Cp*W(NO)(CH_2SiMe_3)(H)(PMe_3) solution was transferred into the NMR tube, which was then evacuated and flame-sealed. Another sample containing *trans*-Cp*W(NO)-(CH_2SiMe_3)(H)(PMe_3) (20.0 mg) was prepared in the same manner. A third sample of *trans*-Cp*W(NO)(CH_2SiMe_3)(H)-(PMe_3) (10.0 mg) was weighed into a vial, and C_6D_6 (0.60 mL) was added via syringe. A phosphate-containing reference capillary was placed into a resealable NMR tube, and then the solution was transferred into the NMR tube. PMe_3 (1.0 μL, 1 equiv) was added via syringe under the flow of Ar. The NMR tube was subsequently evacuated and flame-sealed. For the fourth sample, *trans*-Cp*W(NO)(CH_2SiMe_3)(H)(PMe_3) (10.0 mg) was weighed into a vial, and C_6H_6 (0.6 mL) was added via syringe. A flame-sealed capillary containing tris(4-methoxyphenyl)phosphate with a trace of Cr(acac)$_3$ dissolved in C_6D_6 was added to a resealable NMR tube, and then the

solution containing the organometallic reactant was transferred into the NMR tube, which was evacuated and flame-sealed.

The four unstirred samples were maintained in a 20 °C temperature bath. Spectra were recorded over the course of 55 days with 32 scans and a delay time of 1 s for each ^{1}H NMR spectrum for the first three samples and with 128 scans and a delay time of 35 s for each ^{31}P{^{1}H} NMR spectrum for the fourth sample. For both ^{1}H and ^{31}P{^{1}H} NMR spectra, the resonances due to the starting material and the *cis*-Cp*W(NO)-(C_6D_5)(D)(PMe_3) and Cp*W(NO)(PMe_3)$_2$ products were used to monitor the extent of the reaction after the integrated values of the signals were divided by the integrated values for the resonances of tris(4-methoxyphenyl)phosphate to put them on an absolute scale.

Similarly, *trans*-Cp*W(NO)(CH_2SiMe_3)(H)(PMe_3) (20 mg) was weighed into a vial, and C_6D_6 (0.6 mL) was added via syringe. A flame-sealed capillary containing tris(4-methoxyphenyl)phosphate with a trace of Cr(acac)$_3$ dissolved in C_6D_6 was added to a resealable NMR tube, and then the solution containing the organometallic reactant was transferred into the NMR tube, which was evacuated and flame-sealed. Spectra were recorded over the course of 52 days with 16 scans and a delay time of 17 s for each ^{1}H NMR spectrum and with 98 scans and a delay time of 35 s for each ^{31}P{^{1}H} NMR spectrum. The same procedure was also used for the reactions involving *trans*-Cp*W(NO)(CH_2SiMe_3)(D)(PMe_3) (20 mg) and *trans*-Cp*W(NO)(CH_2CMe_3)(H)(PMe_3) (10 mg), except that these reactions were monitored with 96 scans for ^{31}P{^{1}H}NMR spectra.

X-ray Crystallographic Analysis of Cp*W(NO)(C_6D_5)-(D)(PMe_3). Data collection for this compound was carried out at −100 ± 1 °C on a Bruker X8 APEX diffractometer using graphite-monochromated Mo Kα radiation. Data were collected to a maximum 2θ value of 56.0° in 0.5° oscillations with 30.0 s exposures. The structure was solved by direct methods[17] and expanded using Fourier techniques.[18] All non-hydrogen atoms were refined anisotropically. The metal deuteride hydrogen and the five phenyl deuteriums were refined isotropically as deuterium, while all other hydrogen atoms were included in calculated positions but not refined. The final cycle of full-matrix least-squares refinement on F^2 was based on 4715 observed reflections and 241 variable parameters.

For this structure neutral-atom scattering factors were taken from Cromer and Waber.[19] Anomalous dispersion effects were included in F_c;[20] the values for $\Delta f'$ and $\Delta f''$ were those of Creagh and McAuley.[21] The values for the mass attenuation coefficients are those of Creagh and Hubbell.[22] All calculations were performed using the SHELXTL crystallographic software package of Bruker-AXS.[23] X-ray crystallographic data for this structures are presented in Table 5, and full details of the crystallographic analysis are provided in the Supporting Information.

Theoretical DFT Calculations. To compare the single-point energies of model complexes in a consistent manner, all calculations were carried out using geometries optimized by density functional theory (DFT). Calculations were performed using the Gaussian 03 RevB.04[24] implementation of B3LYP (Becke three-parameter exchange functional (B3)[25] and the Lee−Yang−Parr correlation functional (LYP)[26]) on Intel PIV computers at Kyoto University. A part of the computations was performed on Intel PII computers at the University of British Columbia. Two basis sets were considered. For some preliminary calculations the LanL2DZ basis set that included D95 basis functions for H, C, N, and O[27] and the relativistic electron core potential (ECP) sets of Hay and Wadt for W[28] was employed. The other basis set involved the combination of the Stuttgart−Dresden−Bonn energy-consistent pseudopotential (SDD)[29] for W, the 6-31G basis set for all cyclopentadienyl hydrogen atoms, and the methyl carbon and hydrogen atoms of the PMe_3 ligands and the 6-31G(d,p) basis set for all other hydrogen, carbon, nitrogen, oxygen, and phosphorus atoms. No constraints were imposed on any of the systems. Frequency calculations on optimized species established that all the transition states possessed only one imaginary frequency. Zero-point energy and thermodynamic functions were computed at standard temperature (298.15 K) and pressure (1 atm). Spatial plots of the optimized geometries and frontier

Table 5. X-ray Crystallographic Data for *cis*-Cp*W(NO)(C_6D_5)(D)(PMe_3)

Crystal Data	
empirical formula	$C_{19}H_{24}D_6NOPW$
cryst habit, color	prism, yellow
cryst dimens (mm)	0.35 × 0.15 × 0.10
cryst syst	orthorhombic
space group	$P2_12_12_1$
V (Å^3)	1962.6(4)
a (Å)	10.403(1)
b (Å)	12.984(2)
c (Å)	14.530(2)
α (deg)	90.0
β (deg)	90.0
γ (deg)	90.0
Z	4
formula wt	509.30
calcd density (g/cm^3)	1.724
μ (cm^{-1})	59.71
F_{000}	992.00
radiation	MoKα, 0.710 73 Å
Data Refinement	
final R indices	R1 = 0.011, wR2 = 0.027
goodness of fit on F^2	1.05
largest diff peak and hole (e Å^{-3})	0.60 and −0.53

(17) For SIR92, see: Altomare, A.; Cascarano, M.; Giacovazzo, C.; Guagliardi, A. *J. Appl. Crystallogr.* **1993**, *26*, 343.
(18) Beurskens, P. T.; Admiraal, G.; Beurskens, G.; Bosman, W. P.; Garcia-Granda, S.; Gould, R. O.; Smits, J. M. M.; Smykalla, C. PATTY; University of Nijmegen, Nijmegen, The Netherlands, 1992.
(19) Cromer, D. T.; Waber, J. T. *International Tables for X-ray Crystallography*; Kynoch Press: Birmingham, U.K., 1974; Vol. IV.
(20) Ibers, J. A.; Hamilton, W. C. *Acta Crystallogr.* **1964**, *17*, 781.
(21) Creagh, D. C.; McAuley, W. J. *International Tables of X-ray Crystallography*; Kluwer Academic: Boston, 1992; Vol. C.
(22) Creagh, D. C.; Hubbell, J. H. *International Tables for X-ray Crystallography*; Kluwer Academic: Boston, 1992; Vol. C.
(23) SHELXTL Version 5.1; Bruker AXS Inc., Madison, WI, 1997.
(24) Frisch, M. J.; Trucks, G. W.; Schlegel, H. B.; Scuseria, G. E.; Robb, M. A.; Cheeseman, J. R.; Montgomery, J. A. J.; Vreven, T.; Kudin, K. N.; Burant, J. C.; Millam, J. M.; Iyengar, S. S.; Tomasi, J.; Barone, V.; Mennucci, B.; Cossi, M.; Scalmani, G.; Rega, N.; Petersson, G. A.; Nakatsuji, H.; Hada, M.; Ehara, M.; Toyota, K.; Fukuda, R.; Hasegawa, J.; Ishida, M.; Nakajima, T.; Honda, Y.; Kitao, O.; Nakai, H.; Klene, M.; Li, X.; Knox, J. E.; Hratchian, H. P.; Cross, J. B.; Adamo, C.; Jaramillo, J.; Gomperts, R.; Stratmann, R. E.; Yazyev, O.; Austin, A. J.; Cammi, R.; Pomelli, C.; Ochterski, J. W.; Ayala, P. Y.; Morokuma, K.; Voth, G. A.; Salvador, P.; Dannenberg, J. J.; Zakrzewski, V. G.; Dapprich, S.; Daniels, A. D.; Strain, M. C.; Farkas, O.; Malick, D. K.; Rabuck, A. D.; Raghavachari, K.; Foresman, J. B.; Ortiz, J. V.; Cui, Q.; Baboul, A. G.; Clifford, S.; Cioslowski, J.; Stefanov, B. B.; Liu, G.; Liashenko, A.; Piskorz, P.; Komaromi, I.; Martin, R. L.; Fox, D. J.; Keith, T.; Al-Laham, M. A.; Peng, C. Y.; Nanayakkara, A.; Challacombe, M.; Gill, P. M. W.; Johnson, B.; Chen, W.; Wong, M. W.; Gonzalez, C.; Pople, J. A. *Gaussian 03*, revision B.04; Gaussian, Inc.: Pittsburgh, PA, 2003.
(25) Becke, A. D. *J. Chem. Phys.* **1993**, *98*, 5648.
(26) Lee, C.; Yang, W.; Parr, R. G. *Phys. Rev.* **1988**, *B37*, 785.
(27) Dunning, T. H. J.; Hay, P. J. In *Modern Theoretical Chemistry*; Schaefer, H. F., III, Ed.; Plenum Press: New York, 1976; pp 1−28.
(28) Hay, P. J.; Wadt, W. R. *J. Chem. Phys.* **1985**, *82*, 270. (b) Wadt, W. R.; Hay, P. J. *J. Chem. Phys.* **1985**, *82*, 284. (c) Hay, P. J.; Wadt, W. R. *J. Chem. Phys.* **1985**, *82*, 299.
(29) Dolg, M. In *Modern Methods and Algorithms of Quantum Chemistry*; Grotendorst, J., Ed.; John von Neumann Institute for Computing: Zürich, Switzerland, 2000; Vol. 1, pp 479−508.

orbitals were obtained from Gaussian 03 output using Cambridge Soft Corp.'s Chem 3D Pro v4.0 and Fujitsu WinMOPAC v3.5.

Acknowledgment. We are grateful to the Natural Sciences and Engineering Research Council of Canada for support of this work in the form of grants to P.L. and summer research awards to K.L. We also thank Mr. Xing Jin for providing invaluable technical assistance. P.L. was a 2002−2004 Canada Council Killam Research Fellow.

Supporting Information Available: Full details of crystallographic data as CIF files and tables giving theoretical analyses. This material is available free of charge via the Internet at http://pubs.acs.org.

OM049137E